Secondary shear instability as a source of turbulence in the solar tachocline

By K. Petrovay†

1. Introduction

The tachocline is a thin layer in the interior of the Sun characterized by stable stratification and a strong rotational shear in both the radial and latitudinal directions. This layer is thought to be of crucial importance in the origin of solar activity phenomena. The origin and character of turbulence in this layer is poorly known, even though turbulence has an important role in determining the overall structure of the tachocline. Owing to the strongly stable stratification, the mean radial shear is stable, while the horizontal shear is expected to drive predominantly horizontal, quasi-2D motions in thin slabs. However, here I suggest that a major source of 3D overturning turbulent motions in the tachocline is the secondary shear instability due to the strong, random vertical shear arising between the uncorrelated horizontal flows in neighbouring slabs. A simplified one-dimensional model is presented for the tachocline in this case. It is found that Maxwell stresses due to an oscillatory poloidal magnetic field of a few hundred gauss are able to confine the tachocline to a thickness of a few megameters. The integral scale of the 3D overturning turbulence is the buoyancy scale, on the order of 10 km and its velocity amplitude is a few m/s, yielding a vertical turbulent diffusivity on the order of 10^8 cm^2/s.

The enormous spatial scales of astrophysical flows, such as the flows in stellar interiors and atmospheres, lead to extremely high Reynolds numbers, so these flows are usually strongly turbulent. Studying the flows in the "star in our backyard", the Sun, offers a chance to study turbulent flows in conditions and parameter regimes way beyond the reach of laboratory experiments, terrestrial observations, and often even direct numerical simulations. Further importance to these studies is given by the influence the Sun exerts on the cosmic environment of our planet, determining space weather, and indirectly influencing the terrestrial climate.

The rich variety of solar activity phenomena is the product of a magnetohydrodynamic dynamo operating in the Sun. It is currently thought that a thin layer of the solar interior, known as the tachocline, plays a crucial role in the solar dynamo mechanism, and it can be essentially regarded as the seat of the dynamo. Yet the fluid dynamical properties of this layer are poorly known —in fact even its existence has only been known for little more than a decade, from helioseismic measurements.

From the fluid dynamicist's point of view, the tachocline is an MHD shear flow in the azimuthal direction in a thin, rotating spherical shell with both radial and latitudinal shear and a strongly stable stratification (Richardson number $\sim 10^3$). It is situated at $0.69\,R_\odot$ ($1\,R_\odot = 698$ Mm is the solar radius) and its thickness is less than a few percent of $R_\odot$ (Kosovichev, 1996). There are indications that at high latitudes the tachocline is situated at slightly shallower depths, $r = 0.705 R_\odot$, and it may also be marginally thicker,

† Eötvös University, Department of Astronomy, Budapest, P.O. Box 32, H-1518 Hungary

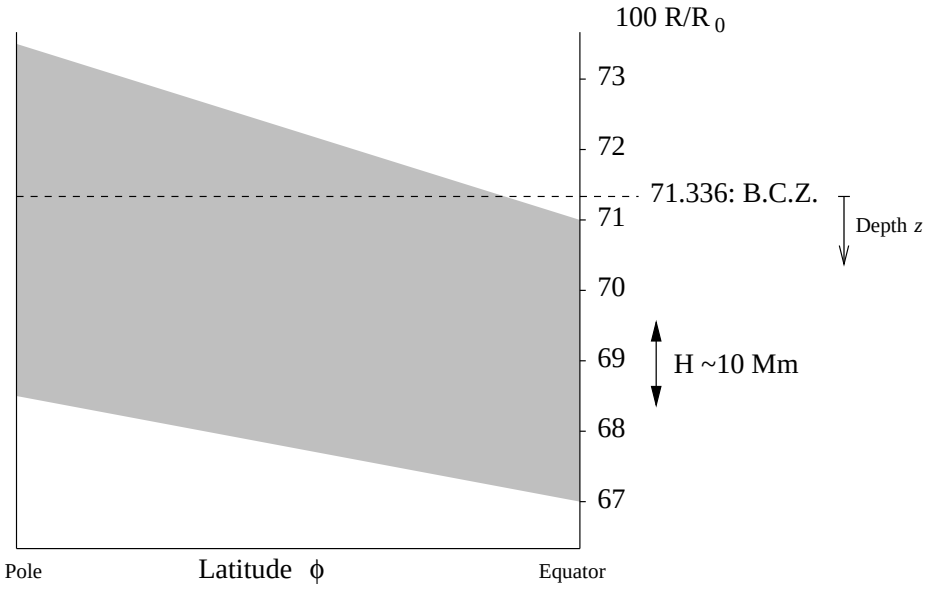

FIGURE 1. Sketch of the geometry of the solar tachocline (proportions distorted)

(Basu & Antia, 2001) —cf. figure 1. The radiative interior below the tachocline rotates like a rigid body, while the convective zone lying above it is characterized by a latitudinal differential rotation which can be regarded independent of depth to a first approximation. The tachocline itself is defined as the transitional layer between these two regimes. The rigid rotation rate of the interior equals the rotation rate of the convective envelope at an intermediate heliographic latitude of about 35°, so the radial shear changes sign at this latitude in the tachocline.

The differential rotation in the convective zone is driven by turbulent angular momentum transport due to nondiagonal terms of the Reynolds stress tensor, which in turn arise as a consequence of the effect of the Coriolis force on turbulence. As pointed out by Spiegel & Zahn (1992), in the absence of turbulence and magnetic fields this differential rotation should penetrate deep ($\sim R_\odot$) into the radiative interior below. The empirical fact that the tachocline is quite thin thus implies the presence of a strongly anisotropic (predominantly horizontal) transport of angular momentum. This may either be due to anisotropic turbulence or to Maxwell stresses in a predominantly horizontal magnetic field. While strongly anisotropic (horizontal) turbulence is the natural expectation in a stably stratified shear layer, the actual calculations (Garaud, 2001*b*; Miesch, 2002) show that the horizontal motions arising from a weak nonlinear instability of the latitudinal shear do not lead to an efficient transfer of angular momentum. This leaves us with magnetic fields as the prime candidate to confine the tachocline to its observed size.

Depending on the value of the magnetic diffusivity, this magnetic field may either be a weak permanent, primordial field pervading the solar interior, or the strong oscillatory

field generated by the solar dynamo. A magnetic field oscillating with a circular frequency $\omega_{\rm cyc} = 2\pi/P$, ($P = 22$ years is the solar cycle period) is known to penetrate a conductive medium only down to a skin depth of

$$H_{\rm skin} = (2\eta/\omega_{\rm cyc})^{1/2} \tag{1.1}$$

where η is the magnetic diffusivity. Basu & Antia (2001) have recently calibrated the thickness of the tachocline: the scale height resulting from their fitting profile is $H \sim 10\,{\rm Mm}$. Accepting this value it follows that for $\eta \lesssim 10^8\,{\rm cm}^2/{\rm s}$ the dynamo field cannot penetrate the tachocline, and we can expect the tachocline to be pervaded by the internal primordial field. On the other hand, for $\eta \gtrsim 10^9\,{\rm cm}^2/{\rm s}$ the tachocline dynamics should be governed by the dynamo field. As the associated diffusive and Lorentz timescales are also very different, these two cases basically correspond to the case of "slow" and "fast" tachocline, discussed in the literature (Gilman, 2000; Brun, 2001).

This shows that turbulence plays a key role in determining the structure of the tachocline. Unfortunately, while the thermal stratification in the tachocline is relatively well known (as summarized in Section 2 below), its fluid dynamical properties, including the precise profile of the rotational flow $v(r,\theta)$, the meridional flow, and the characteristics of turbulence, are very poorly constrained by observations. Direct numerical simulations of stratified shear flows are currently limited to much lower values of the Richardson and Reynolds numbers (Jacobitz & Sarkar, 1998). In consequence, we need to rely on theoretical arguments concerning the properties of turbulent motions in such conditions. On the basis of such arguments, simplified one- or two-dimensional models may be constructed for the mean flow, or appropriate subgrid closure schemes may be constructed for full 3D large-eddy simulations. In the lack of sound theoretical foundations for subgrid closures, all tachocline models published to date have either simply ignored turbulence (Rüdiger & Kitchatinov, 1997, MacGregor & Charbonneau, 1999, Garaud, 2001*a*), or assumed arbitrary fixed scalar turbulent diffusivities in 2D mean flow models (Forgács-Dajka & Petrovay, 2001, Forgács-Dajka & Petrovay, 2002) and in LES (Miesch, 2001, 2002).

The aim of the present work is to attempt to remedy this situation by considering, on the basis of the known stability criteria, the possible sources of turbulence in a strongly stably stratified shear flow with both vertical and horizontal shear, and discussing the expected properties of the turbulence generated by it, on the basis of a dimensional analysis of the K–ϵ equations. As our analysis does not consider the effects of spherical geometry, rotation, or magnetic fields, it should only be regarded as a fist step towards a more comprehensive theoretical analysis of the problem of turbulence in the solar tachocline. These theoretical arguments can be found in Section 3. Then, in Section 4, as an illustration of the use of such theoretical considerations, our prescription for calculating the turbulent diffusivity in the tachocline, equation (3.6), is incorporated in a simplified one-dimensional model for the tachocline. The results show that Maxwell stresses due to an oscillatory poloidal magnetic field of a few hundred gauss (a rather moderate value) are able to confine the tachocline to a thickness of a few megameters. Finally, Section 5 concludes the paper by discussing the implications of this result.

2. Conditions in the tachocline

The thermal stratification of the Sun is quite accurately known from a comparison of standard solar models with helioseismic inversion results. Various characteristic timescales and diffusivities in the tachocline region are plotted in figure 2. As mentioned

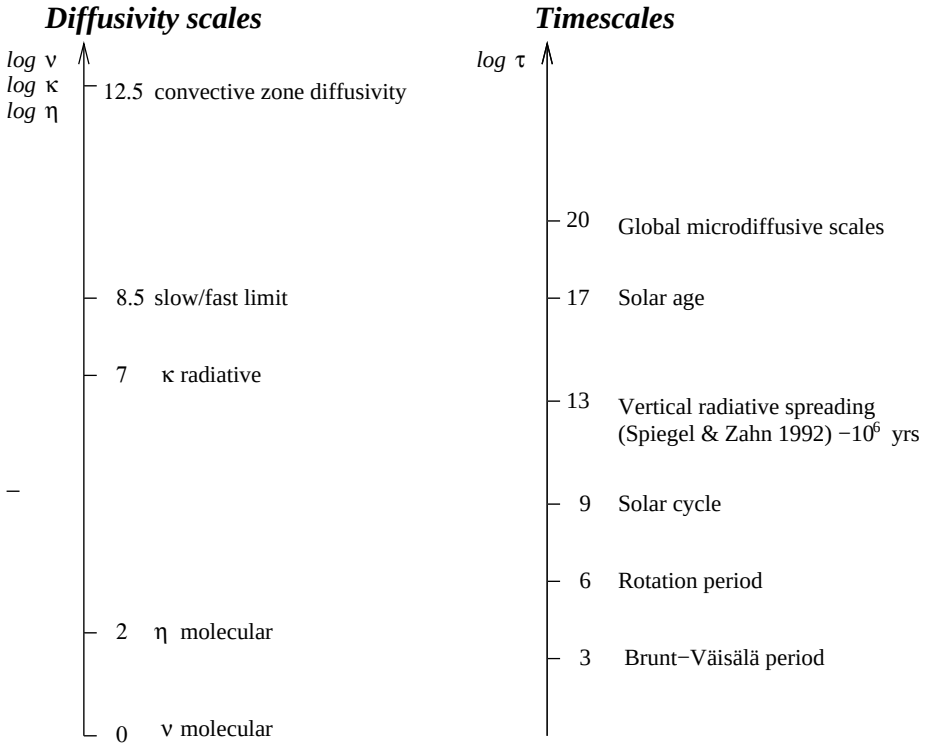

FIGURE 2. Characteristic diffusivities and timescales in the solar tachocline (CGS units)

above, the solar radius is $R_\odot = 698\,\mathrm{Mm}$, the outer 29 % of which comprises the convective zone (CZ). Owing to the high efficiency of convective energy transport, this convective envelope is nearly adiabatically (isentropically) stratified, i.e. the superadiabatic lapse rate $0 < \Delta\nabla = \nabla - \nabla_{\rm ad} \ll 1$.† The radiative interior below the convective zone is characterized by significant negative values of $\Delta\nabla$. For rough estimates, a useful approximation in the tachocline region (i.e. near the top of the radiative zone) is $\Delta\nabla \sim -0.015\,z[\mathrm{Mm}]$, where $z = r_{\rm bcz} - r$ is the depth below the bottom of the convective zone at a radius value of $r_{\rm bcz} = 0.71 R_\odot$. On the other hand, the pressure scale height in this region is $H_P = -P\,dz/dP \sim 50\,\mathrm{Mm}$. With $g = 5\cdot 10^4\,\mathrm{cm^2/s}$, this yields a Brunt-Väisälä frequency

$$N_{\rm BV}^2\,[\mathrm{s}^{-2}] = -\Delta\nabla\frac{g}{H_P} \sim 1.5\cdot 10^{-7}\,z\,[\mathrm{Mm}], \tag{2.1}$$

i.e. in the mid-tachocline, at $z = H \sim 10\,\mathrm{Mm}$ (if the Basu & Antia, 2001, calibration of H is accepted) $N_{\rm BV} \sim 10^{-3}\,\mathrm{s}^{-1}$.

A displaced mass element will then oscillate around its equilibrium position under the action of buoyancy on a timescale $N_{\rm BV}^{-1} \sim 1000\,\mathrm{s}$. The amplitude of the oscillation is

† ∇ is standard astrophysical notation for the lapse rate $d\ln T/d\ln P$.

clearly $\sim v_z/N_{\rm BV}$, so in the presence of turbulent motions, these motions will be limited to a vertical scale $l_b = K^{1/2}/N_{\rm BV}$, called the *buoyancy scale*. ($K = \overline{v_z^2}$ is the kinetic energy in the vertical component of motions.) On the other hand, as an elementary estimate gives $\nu \sim K^2/\epsilon$ for the vertical turbulent diffusivity, one has $l_b \sim (\nu/N_{\rm BV})^{1/2}$. Vertical overturning motions on scales exceeding l_b will be strongly damped by gravity wave emission.

3. The secondary shear instability

The pole-equator difference in the rotational rate of the convective zone is about 30 % of the equatorial rotation rate. Taking half of this value to be the characteristic amplitude of the differential rotation (cf. eq. (3.3) below), we have a differential rotation amplitude of $\Delta v \sim 3 \cdot 10^4$ cm/s at the top of the tachocline. This value is clearly also roughly the amplitude of the vertical velocity difference across the tachocline, so the characteristic vertical shear is

$$S \sim \Delta v/H \sim 3 \cdot 10^{-5}\,{\rm s}^{-1} \tag{3.1}$$

This yields a Richardson number ${\rm Ri} = N_{\rm BV}^2/S^2 \sim 10^3$. This enormous value shows that the vertical shear cannot directly drive turbulence in the tachocline.

Buoyancy, however, cannot stabilize the horizontal shear. While linear stability analysis (Dziembowski & Kosovichev, 1987, Charbonneau *et al.*, 1999) shows that the horizontal shear is marginally stable in the nonmagnetic case, nonlinear effects and magnetic fields are known to lead to instability (Garaud, 2001*b*; Miesch, 2001, 2002). The motions driven by the horizontal shear instability are predominantly horizontal, and their spatial scale is

$$l_h \sim R_\odot, \tag{3.2}$$

while their velocity scale v_h is determined by the amplitude Δv of the horizontal shear at the given depth:

$$v_h \sim \Delta v = R_\odot \frac{[\omega(z, \theta = 0) - \omega(z, \theta = \pi/2)]}{2} \tag{3.3}$$

Overturning turbulent motions in the vertical direction are impeded by the stable stratification, their scale being limited to l_b. Owing to the low vertical diffusivity, however, the horizontal motions will be characterized by a limited vertical correlation length

$$l_c \sim (\nu l_h/v_h)^{1/2}. \tag{3.4}$$

The random horizontal flows driven by the shear will then be limited to thin sheets of thickness l_c, the motion in neighbouring sheets being independent. This will give rise to random vertical shear between neighbouring sheets, of amplitude

$$S_2 \sim v_h/l_c \sim (v_h^3/\nu l_h)^{1/2} \tag{3.5}$$

This *secondary vertical shear* is much stronger than the primary (mean) vertical shear, the corresponding Richardson number being ${\rm Ri}_2 = g\Delta\nabla\nu l_h/H_P v_h^3$. Substituting here the characteristic values of the parameters, we find that ${\rm Ri}_2 < 0.25$, i.e. the secondary shear is unstable, if

$$\nu < \nu_{\rm cr} = \frac{v_h^3}{4 l_h N_{\rm BV}^2} = 10^{-4} \frac{v_h^3[{\rm CGS}]}{z[{\rm Mm}]} \tag{3.6}$$

In the mid-tachocline this value is $\nu_{\rm cr} \sim 10^8\,{\rm cm}^2/{\rm s}$, much higher than the molecular value, so we expect that the secondary shear is strongly unstable.

What is the characteristic amplitude of the turbulent motions driven by the secondary shear instability? In principle, this could be derived from a K–ϵ model (or, more, generally, from a Reynolds stress model —cf. Mansour, Kim & Moin, 1999). Assuming plane parallel geometry for simplicity, the relevant equations are of the general form

$$\frac{\partial K}{\partial t} = P_K - D_K - \frac{\partial F_K}{\partial z} \tag{3.7}$$

$$\frac{\partial \epsilon}{\partial t} = P_\epsilon - D_\epsilon - \frac{\partial F_\epsilon}{\partial z} \tag{3.8}$$

Here, the non-local fluxes or third order moments (TOMs) are

$$F_K = \overline{v_z^3} \tag{3.9}$$

$$F_\epsilon = \overline{v_z \epsilon_l} \tag{3.10}$$

ϵ_l being the local dissipation rate, while ϵ is the mean dissipation. The production terms are usually modelled as

$$P_K = \frac{\nu}{2} S_2^2 \tag{3.11}$$

$$P_\epsilon = C_P \frac{\epsilon}{K} P_K \tag{3.12}$$

while, assuming an ideal gas and the Boussinesq approximation $\rho'/\rho = -T'/T$ (prime denotes fluctuations), the dissipation/sink terms read

$$D_K = \epsilon + g\overline{v_z T'} \tag{3.13}$$

$$D_\epsilon = C_{D1} \frac{\epsilon^2}{K} + C_{D2} \frac{\epsilon}{K} g\overline{v_z T'} \tag{3.14}$$

(The first terms on the r.h.s. represent viscous dissipation, while the second terms correspond to gravity wave emission. Note that in a subadiabatic environment $\overline{v_z T'} > 0$, i.e. downmoving fluid parcels are hotter than average.)

Performing a dimensional analysis on these equations we find that the diffusive timescale, corresponding to the non-local terms, is $d^2/\nu \gtrsim d^2/\nu_{\rm cr} \sim 10^{10}\,{\rm s}$, while the timescale associated with the shear production term is $K/\nu S_2^2 \sim N_{\rm BV}/S_2^2 \sim N_{\rm BV} l_h \nu / v_h^3 \sim 10^{-5}\nu < 10^3\,{\rm s}$. This implies that the transport terms can be neglected in the K-ϵ equations. Under such conditions the equations have no stationary solution, as the values of the constants C_P, C_{D1} and C_{D2} are different in general. The intensity of turbulence will then keep increasing until the turbulent diffusivity reaches the critical value $\nu_{\rm cr}$, when further shear production is switched off.

We thus conclude that the secondary vertical shear instability can be expected to drive overturning turbulence to the level $\nu = \nu_{\rm cr}$ on a short timescale. The turbulence generated by this mechanism may then be crudely represented by the vertical diffusivity value given by eq. (3.6).

4. Tachocline model

We now proceed to develop a simple one-dimensional model for the solar tachocline, assuming that the secondary shear instability discussed in the previous section is the

only source of turbulence in the tachocline region. Our computational domain will be restricted to the top of the radiative interior, below $r_{\rm bcz}$.

From figure 2 it is apparent that the convective zone is characterized by extremely high turbulent diffusivities. Due to the Coriolis force, the Reynolds stress tensor also has significant nondiagonal components in the convective envelope. These components imply an angular momentum transport which is thought to be the main driver of solar differential rotation. Based on the discussion of the previous section we expect that the amplitude of turbulence in the tachocline is much lower than in the CZ. Thus, from the point of view of tachocline modelling, it is not unrealistic to regard the latitudinal differential rotation at $r = r_{\rm bcz}$ as a given boundary condition imposed at the top of the region of interest. This is tantamount to assuming that differential rotation is driven by a highly effective mechanism in the convective zone which is not seriously influenced by the processes in the tachocline.

As the layer studied is thin, we also adopt a plane parallel representation for it, with constant density. (The effects of density stratification are only implicitly taken into account by its role in determining the turbulent viscosity, eq. (3.6).)

Thus, we regard the following model problem. Consider a plane parallel layer of incompressible fluid of density ρ, where the viscosity ν and the magnetic diffusivity η depend on z only. At $z = 0$ where z is the vertical coordinate (corresponding to depth in the solar application we have in mind) a periodic horizontal shearing flow is imposed in the y direction:

$$v_{y0} = v_0 \cos(kx)$$

(so that x will correspond to heliographic latitude, while y to the longitude). We assume a two-dimensional flow pattern ($\partial/\partial y = 0$) and $v_x = v_z = 0$ (no "meridional flow"). An oscillatory horizontal "poloidal" field is is present in the x direction, given by

$$V_p = \frac{1}{(4\pi\rho)^{1/2}} \frac{\partial A}{\partial z} \tag{4.1}$$

(in Alfvénic units). The "toroidal" (i.e. y) component A of the vector potential obeys the corresponding component of the integral of the induction equation, which in our case simplifies to a diffusion equation:

$$\frac{\partial A}{\partial t} = \frac{\partial}{\partial z}\left(\eta \frac{\partial A}{\partial z}\right) \tag{4.2}$$

The upper boundary condition $A = A_0$ at $z = 0$ fixes the poloidal field amplitude.

The evolution of the azimuthal components of the velocity and the magnetic field is described by the corresponding components of the equations of motion and induction, respectively. Introducing $v = v_y$ and using Alfvén speed units also for the toroidal magnetic field

$$b = B_y (4\pi\rho)^{-1/2}, \tag{4.3}$$

these can be written as

$$\frac{\partial v}{\partial t} = V_p \cos(\omega t) \frac{\partial b}{\partial x} + \frac{\partial}{\partial z}\left(\nu \frac{\partial v}{\partial z}\right) \tag{4.4}$$

$$\frac{\partial b}{\partial t} = V_p \cos(\omega t) \frac{\partial v}{\partial x} + \frac{\partial}{\partial z}\left(\eta \frac{\partial b}{\partial z}\right) \tag{4.5}$$

where we have taken into account that, owing to the thinness of the tachocline, the

vertical derivatives dominate the diffusive terms. As the imposed poloidal field V_p is independent of x, Fourier transforming (4.4) and (4.5) in terms of x yields the same equations for the Fourier amplitudes $\hat{v}$ and $\hat{b}$, except that $\partial/\partial x$ is substituted by ik:

$$\frac{\partial v}{\partial t} = ikbV_p \cos(\omega t) + \frac{\partial}{\partial z}\left(\nu \frac{\partial v}{\partial z}\right) \tag{4.6}$$

$$\frac{\partial b}{\partial t} = ikvV_p \cos(\omega t) + \frac{\partial}{\partial z}\left(\eta \frac{\partial b}{\partial z}\right) \tag{4.7}$$

(Hats are omitted to simplify notation.) For a rough estimate, we write $\pi b/P$ for the l.h.s. of (4.7), then substitute the resulting expression of b into (4.6), take the real part, and omit the factor $\cos^2(\omega t)$ in the first term on the r.h.s.:

$$\frac{\partial v}{\partial t} = -k^2 V_p^2 P v + \frac{\partial}{\partial z}\left(\nu \frac{\partial v}{\partial z}\right) \tag{4.8}$$

The equations to solve are thus (4.1), (4.2) and (4.8), with the turbulent diffusivities $\nu = \eta = \nu_m + \nu_{\rm cr}$ given by equation (3.6) with the identification $v_h = v$. ν_m is a minimal diffusivity value ("molecular diffusivity").

The simplified form of the first term in equation (4.8) will not allow a correct reproduction of the periodic part of the time dependence. The important point is, however, that this sink term, representing the reduction of horizontal shear by Maxwell stresses, has the right amplitude and the correct scaling with V_p, P, v, and k, so it may be expected to reproduce well the cycle-averaged flow amplitude as a function of z, which is our main interest here. Indeed, solving our equations for the case of constant diffusivities ν and η, the results are in a remarkably good agreement with the fully consistent solutions in spherical geometry, presented in Forgács-Dajka & Petrovay (2002).

The equations were solved numerically by a finite difference scheme second-order accurate in time. All quantities were set to zero at the lower boundary, situated at $z_0 = 60$ or 30 Mm below $r_{\rm bcz}$, while the boundary conditions applied at top ($z = 0$) were $v = v_0 = 3 \cdot 10^4$ cm/s and different prescribed values for A_0. As equation (3.6) is singular at $z = 0$, ν was set to a high finite value $\nu_{\max}$ here. For ν_m we used the value 10^7 cm^2/s. This is much higher than the actual molecular diffusivities in the tachocline, but using a realistic value would lead to forbiddingly long integration times. Similarly, a too high value for $\nu_{\max}$ would lead to very short timesteps, also increasing the computing time to unaffordable values. Test runs with varying values of $\nu_{\max}$ and ν_m, however, show that these choices do not significantly distort the results.

Starting from an arbitrary initial state, the system was allowed to evolve until very nearly periodic behaviour sets in (in about 10^4 years, depending on the value of ν_m), then average quantities for one 11-year half-cycle were computed and plotted as functions of depth (Figs. 3 and 4).

5. Discussion

In the case with a very weak magnetic field (left-hand column in figure 3), it is straightforward to show that equation (4.8) with ν given by (3.6) admits the analytic solution

$$v = v_0 \left[1 - \left(\frac{z}{z_0}\right)^2\right]^{1/4}, \tag{5.1}$$

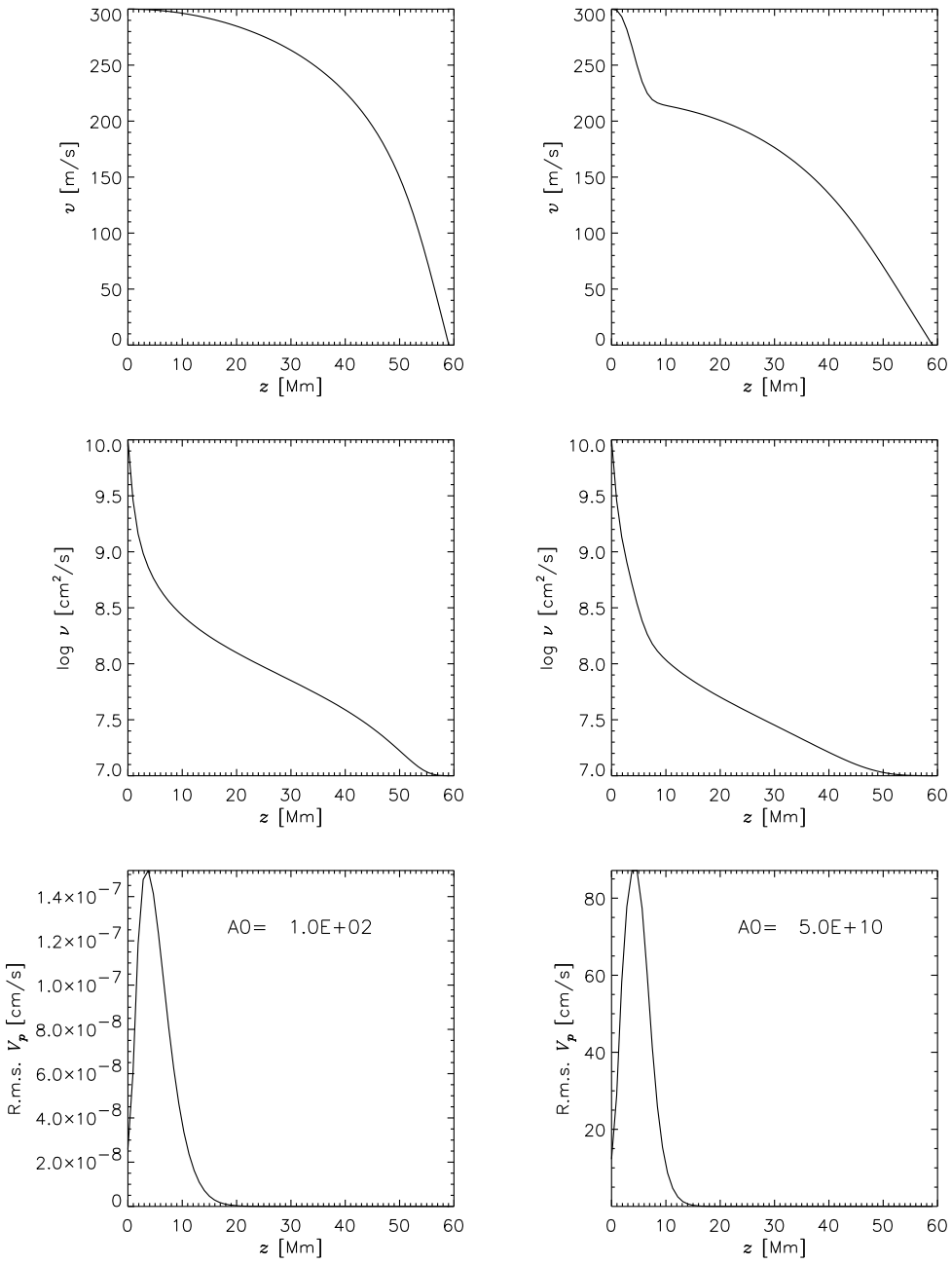

FIGURE 3. Horizontal differential rotation amplitude $v = v_h$, as defined in eq. (3.3) *(top row)*, vertical turbulent diffusivity ν *(middle row)*, and poloidal magnetic field in Alfvenic units *(bottom row)*, averaged over a solar half-cycle, as functions of depth below the convective zone, for a very low *(left-hand column)* and a medium *(right-hand column)* value of the field strength imposed at the top. Note that by coincidence, in the solar tachocline the field strength in gauss is roughly equal to the corresponding Alfven speed in cm/s.

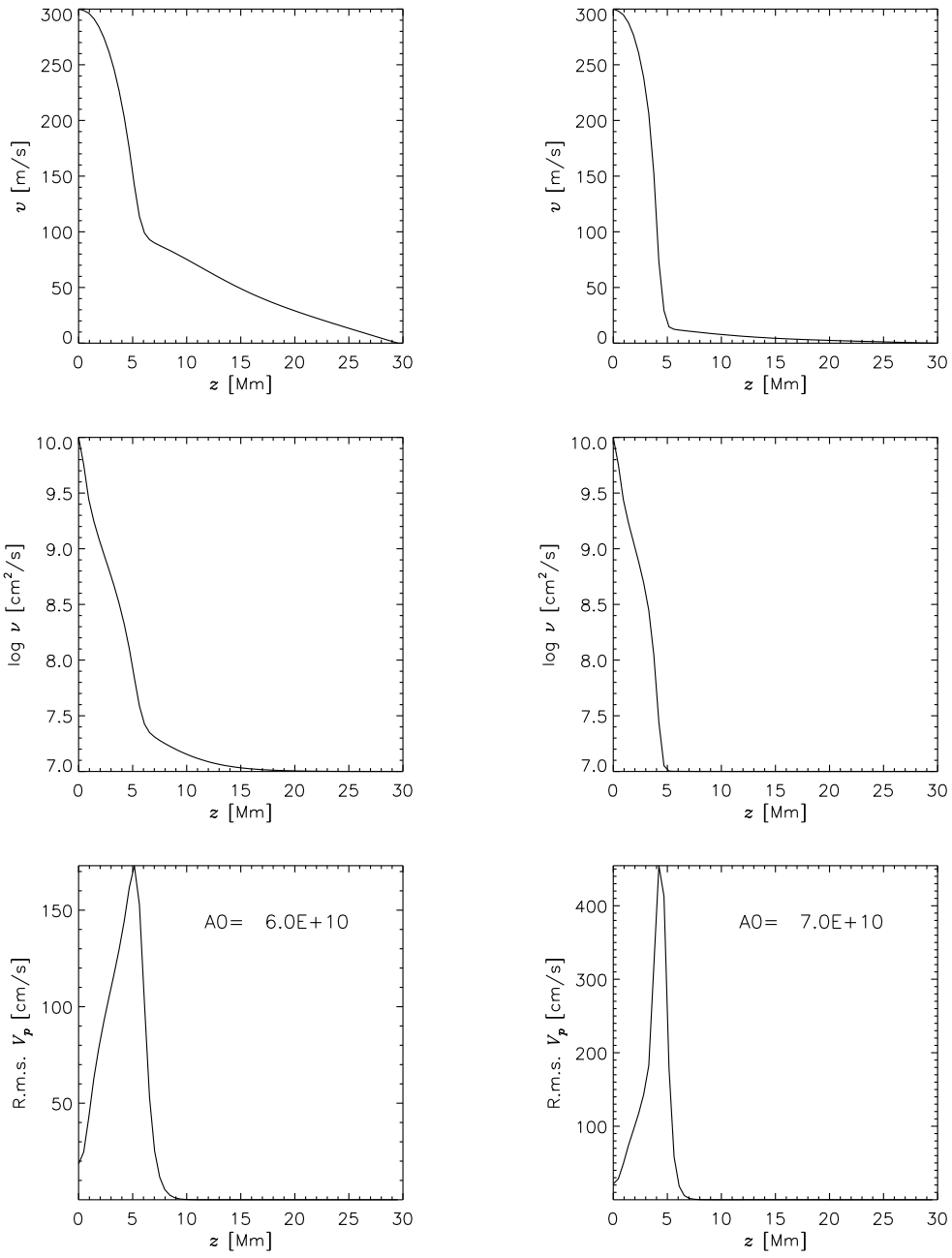

FIGURE 4. Same as figure 3 for two higher field strength values.

confirmed by the numerical calculations. This essentially means that in this case the shear penetrates as far down into the radiative interior as the placement of the lower boundary condition allows. The weak magnetic field itself only penetrates down to the skin depth given by equation (1.1), as expected. It is worth noting that the poloidal field

shows a non-monotonic behaviour with depth in all cases, reaching its maximum at some finite z value. This is due to the variable diffusivity: the horizontal field lines tend to "pile up" where the diffusivity is significantly reduced.

From the right-hand column of figure 4 we can see that a poloidal magnetic field of a few hundred gauss (peak strength 500 G) can confine the tachocline to a thickness of barely 4 Mm. This field strength is quite realistic: the total poloidal flux in the tachocline in this case is comparable to the flux through the solar surface, as required. Nevertheless, the resulting thin tachocline seems to be at odds with the results of Basu & Antia (2001), and is also hard to reconcile with the gradual depletion of lithium in the atmospheres of Sun-like stars during their lifetimes. Lithium is destroyed by nuclear reactions in layers below $z \sim 40\,\mathrm{Mm}$ only, so a mixing characterized by a diffusivity of at least $10^3\,\mathrm{cm}^2/\mathrm{s}$ must be present as far down as that depth. While our prescription $\nu_m = 10^7\,\mathrm{cm}^2/\mathrm{s}$ does not allow a firm statement on this issue, the very sharp cutoff of the ν-curve in the figures under discussion does not seem to indicate that any significant level of turbulence could be maintained at such great depths.

One might think that an intermediate field strength might lead to a somewhat thicker tachocline. This is, however, not the case: an inspection of the full series of results in our figures clearly shows that a weaker field simply results in an "aborted tachocline", i.e. the horizontal shear is first reduced by a factor depending on the field strength in a thin layer of a few Mm, but below that layer, as the magnetic field is damped by the skin effect, it follows the field-free solution (5.1), with a lower amplitude. It remains to be seen, whether such a two-tiered v-profile can yield an equal or better fit to helioseismic data than the more conventional profiles, used e.g. by Basu & Antia (2001).

One obvious shortcoming of the present models is their simplified treatment of the time development and of the geometry. The development of more realistic, axially symmetric spherical models employing the viscosity formula (3.6) is in progress.

Acknowledgements

I thank Nagi Mansour, Sasha Kosovichev, and Alan Wray for their warm hospitability during my stay at Ames. This paper owes much to discussions with them and with Mark Miesch. This work was supported in part by the OTKA under grant no. T032462.

REFERENCES

Basu, S. & Antia, H. M. 2001 A Study of Possible Temporal and Latitudinal Variations in the Properties of the Solar Tachocline. *Mon. Not. Roy. Astr. Soc.* **324**, 498–508.

Brun, A. S. 2001 In *Helio- and Asteroseismology at the Dawn of the Millennium*, p. 273. ESA Publ. SP-464.

Charbonneau, P., Dikpati, M. & Gilman, P. A. 1999 Stability of the Solar Latitudinal Differential Rotation Inferred from Helioseismic Data. *Astroph. J.* **526**, 523–537.

Dziembowski, W. & Kosovichev, A. 1987 Low Frequency Oscillations in Slowly Rotating Stars III: Kelvin-Helmholtz Instability. *Acta Astr.* **37**, 341.

Forgács-Dajka, E. & Petrovay, K. 2001 Tachocline Confinement by an Oscillatory Magnetic Field. *Solar Phys.* **203**, 195–210.

Forgács-Dajka, E. & Petrovay, K. 2002 Dynamics of the Fast Solar Tachocline I: Dipolar Field. *Astron. Astroph.* **389**, 629–640.

Garaud, P. 2001*a* Dynamics of the Solar Tachocline I: An Incompressible Study. *Mon. Not. Roy. Astr. Soc.* **329**, 1–18.

Garaud, P. 2001*b* Latitudinal Shear Instability in the Solar Tachocline. *Mon. Not. Roy. Astr. Soc.* **324**, 68–76.

Gilman, P. A. 2000 Fluid dynamics and mhd of the solar convection zone and tachocline: Current understanding and unsolved problems. *Solar Phys.* **192**, 27–48.

Jacobitz, F. G. & Sarkar, S. 1998 The effect of nonvertical shear on turbulence in a stratified medium. *Phys. Fluids* **10**, 1158–1168.

Kosovichev, A. G. 1996 Helioseismic Constraints on the Gradient of Angular Velocity at the Base of the Solar Convection Zone. *Astroph. J.* **469**, L61–L64.

MacGregor, K. B. & Charbonneau, P. 1999 Angular Momentum Transport in Magnetized Stellar Radiative Zones. IV. Ferraro's Theorem and the Solar Tachocline. *Astroph. J.* **519**, 911–917.

Mansour, N. N., Kim, J. & Moin, P. 1989 Near-Wall k–ϵ Turbulence Modeling. *AIAA Journal* **27**, 1068–1073.

Miesch, M. S. 2001 Numerical Modeling of the Solar Tachocline. I. Freely Evolving Stratified Turbulence in a Thin Rotating Spherical Shell. *Astroph. J.* **562**, 1058–1075.

Miesch, M. S. 2002 Numerical Modeling of the Solar Tachocline. II. Forced Turbulence with Imposed Shear. *Astroph. J.* to be published

Rüdiger, G. & Kitchatinov, L. L. 1997 The Slender Solar Tachocline: A Magnetic Model. *Astr. Nachr.* **318**, 273–279.

Spiegel, E. A. & Zahn, J.-P. 1992 The Solar Tachocline. *Astron. Astroph.* **265**, 106–114.